Journal of Additive Manufacturing Technologies
DOI: 10.18416/JAMTECH.2111549

Infinite Science | Publishing

A numerical investigation of the effect of support thickness and void ratio on thermal behavior and possible martensite decomposition in laser powder-bed fusion process

A.K. Yildiz[1], M. Mollamahmutoglu[1], E. Dogan[1*], and O. Yilmaz[1]

[1] Advanced Manufacturing Technologies Research Group (AMTRG), Department of Mechanical Engineering, Faculty of Engineering, Gazi University, Maltepe, 06570 Ankara, Turkey,
[*] Corresponding author, email: ebubekir.dogan@gazi.edu.tr

Abstract

Laser powder-bed fusion allows the production of complex parts. However, the thermal nature of the process involves spatially and rapidly changing heating-cooling cycles. This type of thermal process causes the formation of highly martensitic microstructures with poor ductility and crack resistance. To overcome this issue, a more lamellar structure for improved physical properties can be obtained either by an approach during production or by a post-production heat treatment. In this context, the support structure together with the substrate temperature are factors that can make a difference during production. If these two factors are properly determined by an assessment prior to production, martensite decomposition can be achieved.

In this study, the effect of the thickness and void ratio of a support structure with a constant cross-sectional area on the thermal behaviour of the process was investigated numerically for the Ti6Al4V alloy. For this purpose, a case is examined for different void ratios and support thicknesses. As a result, it has been presented that the support structure, together with suitable laser parameters, cooling time and substrate temperature, can help the decomposition of the martensitic structure.

Keywords: Laser powder bed fusion, Simulation, Support thickness, Support void ratio, Martensite decomposition.

1. Introduction

Laser powder-bed fusion (LPBF) is widely used in the additive manufacturing of metals. This method is particularly suitable for the production of dimensionally small but detailed parts. It has become popular due to some advantages such as flexibility and reducing material waste. On the other hand, there are some concerns with mechanical properties as well as problems such as porosity and surface quality [1]. The microstructures are primary factors to determine the mechanical properties of the manufactured parts. They form as a result of thermal history and related stresses.

The thermal nature of the production is quite complex due to the rapid melting and fusion of the metal powders by a laser with a small beam diameter and intense energy. Since the manufacturing process is accomplished by the fusion of hot small masses to relatively colder masses, high temperature gradients and cooling rates are observed. In addition, the sequential scanning of the relevant region by the laser causes a spot to experience several heating-cooling cycles. As a result of this type of manufacturing, parts with a high martensitic microstructure are generally produced, and such martensitic structures are very brittle [2], [3].

As mentioned above, lamellar structures composed of alpha-beta may be desired instead of these brittle structures. If it is aimed to obtain this lamella structure during production, various approaches can be made. For example, as in selective electron beam melting (SEBM), the build chamber can be kept at a high temperature at all times and then allowed to cool slowly. Another approach may be to control the cooling of the material with secondary heat sources. Both approaches have pros as well as cons. Another interesting approach, which is the subject of this study, is martensite decomposition. It does not require a special vacuum environment as in SEBM. The method benefits from more efficient use of the existing heat source instead of a secondary heat source. It is tempting that the energy to be used anyway for the fusion serves a secondary purpose. In fact, some studies are available to obtain better mechanical properties [4], [5].

Martensite decomposition is based on the principle of transforming the formed martensitic structures back into a lamellar structure after a certain period of time, using the heat input as a result of successive scanning at the upper layers [6]. While this idea is interesting, it is challenging as it requires tools and accurate calculations to control and predict the thermal process.

Support structures are important in the context of process control. Because most of the energy flows in the substrate direction through the support structures. Therefore, support structures, together with appropriate laser parameters, cooling time and substrate temperature, can allow martensite decomposition. In this study, the effect of support thickness and void ratio on the thermal process was analyzed numerically. In order to indicate the effect, three different void ratios and support thicknesses were tested.

2.Theory

2.1 The thermal behavior of the process

The macro-scale cross-sectional representation of the thermal process is given in Figure 1. Here, laser energy as a heat source exists on the upper surface. A portion of this energy can be considered as rejected from the surface due to the reflection and spattering effects, while the remainder will be absorbed by the material. In addition, convection, radiation and evaporation heat losses on the upper surface can be mentioned.

The part produced is surrounded by powder with low thermal conductivity. On the lower surface, there is the substrate kept at the same temperature by the system. Above the substrate, there is a support with a thickness of H and a void ratio of β. Here, A denotes the scanning area and is taken to be constant for both the support and the part, as previously stated. l is the powder layer thickness, and the effective layer thickness is less than this value as a result of melting and coalescence.

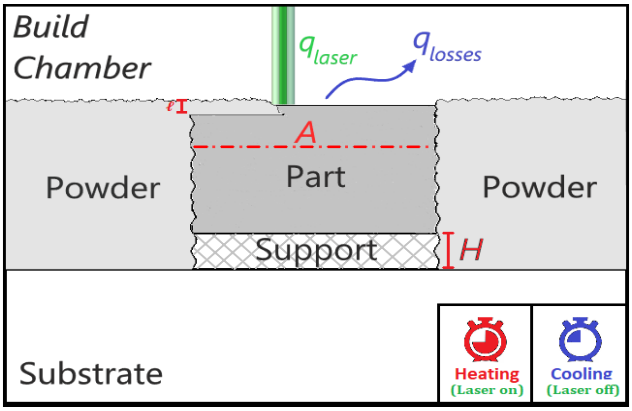

Fig 1. Cross-section schematic of the process.

Most of the heat absorbed by the system flows towards the substrate. Thus, the substrate temperature and support structure are important in terms of cooling behavior. In addition, the cooling period, which starts with the shutdown of the laser and includes powder spreading, is another important factor. In fact, the cooling for a spot begins immediately after the laser has moved far enough from a region in the scanning area. Factors that may affect the thermal process are summarized in Table 1.

2.2. Governing equations, process parameters and thermophysical properties

The general 3D heat transfer can be expressed as follows:

Table 1. Factors that may affect the thermal process.

Thermophysical properties of materials	Bulk and powder forms of metal, protective noble gas
Laser properties	Max. power, beam diameter, wave length
Scan parameters	Power, scan speed, scan strategies, nominal powder layer thickness
Build chamber conditions	Surrounding (chamber walls), substrate and ambient temperatures
Dimensional conditions	Part and support dimensions
Cooling time	Waiting and powder spreading times

$$\rho c \frac{\partial T}{\partial t} = \frac{\partial}{\partial x}\left(k_x \frac{\partial T}{\partial x}\right) + \frac{\partial}{\partial y}\left(k_y \frac{\partial T}{\partial y}\right) + \frac{\partial}{\partial z}\left(k_z \frac{\partial T}{\partial z}\right) + Q(x, y, z, t) \quad (1)$$

where ρ, c, k, and T are the density (kg m^{-3}), heat capacity (J kg^{-1} K^{-1}), anisotropic conductivity (W m^{-1} K^{-1}), and temperature (K), respectively. If required, enhanced factors can also be used for anisotropic conductivity:

$$k_x = k_{bulk}\lambda_x, k_y = k_{bulk}\lambda_y, k_z = k_{bulk}\lambda_z \quad (2)$$

Convection and radiation losses for part and powder surfaces in the building chamber are given in equations 3 and 4, respectively.

$$q_c = h\,(T - T_{amb}) \quad (3)$$

$$q_r = \varepsilon\sigma\,(T^4 - T_{sur}^4) \quad (4)$$

Here, h, ε and σ are convective heat transfer coefficient (W m^{-2} K^{-1}), emissivity and Stefan-Boltzmann constant (5.67 10^{-8} W m^{-2} K^{-4}), respectively. The heat source is expressed as a 2D gaussian distribution:

$$q = \frac{2\alpha P}{\pi r^2}\exp\left(-\frac{2(x^2+y^2)}{r^2}\right) \quad (5)$$

Here, P is the laser power (W), and α represents absorptivity.

The model has been realistically designed as multi-scan and multi-layer and built in the Comsol program. Material hysteresis (powder to solid transformation) is also taken into account. Such that, since the powder material properties differ from those of bulk/solidified material, the transformation is defined in a separate physics as the liquefaction field variable for the domain.

An appropriate parameter set was determined as a result of preliminary trial and error. The absorptivity

was chosen based on a previous study [7]. The correlation in the study was modified and used by considering the beam diameter ratios. The obtained absorption value indicates that the keyhole regime has not been entered. Because the keyhole regime absorption value is expected to exceed 0.4. As a result, it was not necessary to increase the anisotropic conductivity values in equation 2 in order to express effects such as Marangoni and recoil pressure. General information relevant to the case is presented in Table 2.

Table 2. Case parameters.

Laser power [W]	350
Scan speed [mm s^{-1}]	1000
Beam diameter [µm] ($1/e^2$)	180
Powder porosity [-]	0.5
Nominal powder layer thickness [µm]	60
Effective solidified layer thickness [µm]	30→60
Hatch distance [µm]	120
Initial, substrate and surrounding temperature [K]	473
Absorptivity [-]	0.375
Anisotropic enhanced factors [-]	λ_x= λ_y= λ_z=1 (no enhancement)
Convective heat transfer coefficient [W m^{-2} K^{-1}]	10
Scanning area [mm^2]	20 (5x4) (41 tracks)
Scan strategy [-]	Zigzag
Cooling time [s]	1

Table 3. Material properties of Ti6Al4V alloy.

Physical Properties	Value
Solidus temperature T_S (K)	1877
Liquidus temperature T_l (K)	1923
Beta transus temperature T_β (K)	1268
Solid specific heat capacity C_{ps} (J kg^{-1} K^{-1})	483.04+0.215T, T≤1268 412.7+0.1801T, 1268<T≤1923 [8]
Liquid specific heat capacity C_{pl} (J kg^{-1} K^{-1})	831 [8]
Solid thermal conductivity k_s (W m^{-1} K^{-1})	1.25+0.015T, T≤1268 3.15+0.012 T, 1268< T≤1923 [8]
Liquid thermal conductivity k_l (W m^{-1} K^{-1})	-12.75+0.024T, T>1923 [8]
Powder thermal conductivity k_p (W m^{-1} K^{-1})	0.0014*T+0.2204, T<1923[9]
Density ρ (kg m^{-3})	4200
Latent heat of fusion L (kJ kg^{-1})	286
Emissivity ε	0.6, T≤1500 0.4, T>1500 [10]
Convection heat transfer coefficient h_c	10 W m^{-2} K^{-1}

Ti6Al4V alloy was chosen for the case. The temperature-dependent properties used in the model are given in Table 3.

3. Results and discussion

Figure 2 shows a 3D schematic of the domain and a 2D schematic of the scanning area. Here, the temperature at the P point in the center of the scanning area will be monitored. This point will be affected periodically by adjacent scans and successive new layers. This approach provides convenience in the context of examining the general behavior of the process and martensitic decomposition. However, it should be mentioned that the cooling of the points close to the surface would be faster. For one second cooling time, a scanning area of 20 mm was considered sufficient for martensite decomposition to occur. For a more realistic cooling time of 5-10 seconds, a larger area may be sufficient. In any case, the points near the surface of the part will usually be martensitic as they cool rapidly. In addition, a certain number of new layers are required for martensite decomposition to begin at the p point. Thus, the last layers (uppermost) will also be of martensitic structure. Because there will not be upper layers to enable their transformation.

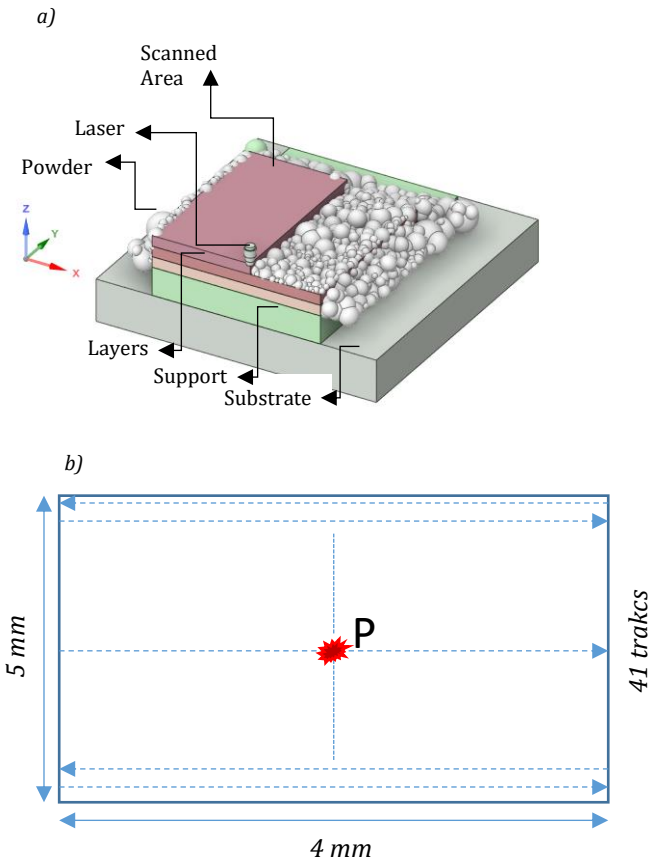

Fig 2. 3D schematic of the domain cross-section (a), 2D schematic of the scanning area and scan strategy (b).

In order to compare the effect of the support structure, three different void ratios (β = 0, 0.5, 0.75) were evaluated for the 2 mm thickness. Then, two different thicknesses (H = 0.5 mm, 4 mm) were calculated for the void ratio of 0.75. Since the change in the P point showed a monotonous behavior after the sixth layer, the calculation cost was reduced by extrapolation. As a result, a total of approximately 100 hours of calculation was performed for five separate cases with six new layers.

The detailed thermal history of the P point is presented in Figure 3 as an example case. As can be seen, the temperature is periodically affected by adjacent scans and successive layers, but this influence fades away. The jump in temperature as a result of scanning and cooling is reduced. Thus, a kind of bridge can be formed by combining the minimum temperatures reached for each new layer.

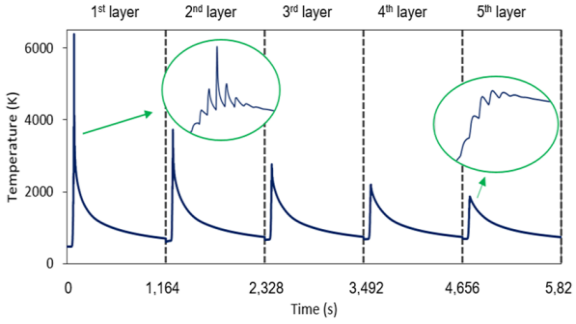

Fig 3. Thermal history of Point P (Case: β = 0.75, H = 2mm).

Thermal bridges formed for five cases are presented in Figure 4. As can be seen, as the void ratio increases for a thickness of 2 mm, heat accumulation can be achieved in the system. The new layers can even provide the martensite decomposition temperature for the 0.75 void ratio. On the other hand, the decrease of the support thickness to 0.5 mm for 0.75 void ratio seriously affects the system. The system cools down rapidly and approaches the substrate temperature, and there cannot be heat accumulation. 4 mm allows the point P to reach higher temperatures. Consequently, for a void ratio of 0.75, support thicknesses of 2 and 4 mm can initiate martensite decomposition at point P.

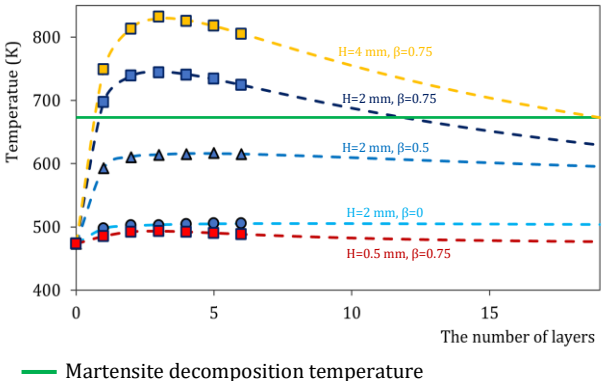

Fig 4. Temperature behavior at point p for different support structures.

The martensite decomposition temperature can be considered as a first condition. However, it does not guarantee decomposition. Around this temperature, the cooling rate should be low enough. In brief, the newly added layers should allow the temperature to decrease slowly at the P point. Before falling below the martensite decomposition temperature, the cooling rate must drop below the critical cooling rate [11].

In Figure 5, the cooling rates are given for two cases where martensite decomposition may occur. As can be seen, the cooling rate is below the critical rate at the eleventh layer. In both cases, decomposition can occur because the temperature does not fall below the critical temperature. However, it can be considered that it will be more comfortable for the 4 mm thickness. Because it has met this condition long before it reaches the decomposition temperature.

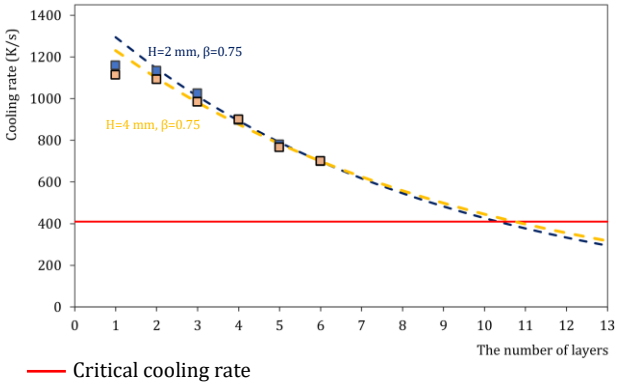

Fig 5. Cooling rates for the cases β = 0.75, H = 2 mm, 4mm.

Consequently, support structures can be helpful in microstructure tailoring. However, some limitations and disadvantages should also be considered. The main one of them is the distortion that may occur as a result of thermal processing. This issue must be addressed to achieve an ideal production. Furthermore, design evaluations should be conducted in the context of time and powder use.

4. Conclusions

- The support structures are preferred is to prevent situations such as flowing and distortions of the manufactured part. As a further situation, it would be possible to tailor the microstructure by the optimization of these structures. The support structures formed between the part and the substrate deserve special attention as they control the transfer rate of heat to the substrate. Therefore, these structures can play an auxiliary role in obtaining some desired mechanical properties in some cases.

- In this study, the effects of the support structure on the thermal process are shown for the same process parameters. It has been observed that the thermal history and cooling rates of the layers are affected by the thickness and void ratio of a support structure with a constant cross-sectional area. The support structure may further allow martensite decomposition in some sections, allowing a lamellar microstructure. In this

context, this study contributes to the consideration of support structures from another perspective.

Author's statement

Ayşe Kübra Yıldız: Conceptualization, Methodology, Software, Formal analysis, Investigation.

Mehmet Mollamahmutoğlu: Conceptualization, Methodology, Formal analysis, Writing - Original Draft, Writing - Review & Editing.

Ebubekir Doğan: Writing - Review & Editing, Visualization.

Oğuzhan Yılmaz: Conceptualization, Resources, Writing - Review & Editing, Supervision, Project administration.

Conflict of interest: Authors state no conflict of interest. Informed consent: Informed consent has been obtained from all individuals included in this study. Ethical approval: The research related to human use complies with all the relevant national regulations, institutional policies and was performed in accordance with the tenets of the Helsinki Declaration, and has been approved by the authors' institutional review board or equivalent committee.

References

1. Acharya, R., J.A. Sharon, and A. Staroselsky, *Prediction of microstructure in laser powder bed fusion process.* Acta Materialia, 2017. **124**: p. 360-371.
2. Sing, S.L., S. Huang, and W.Y. Yeong, *Effect of solution heat treatment on microstructure and mechanical properties of laser powder bed fusion produced cobalt-28chromium-6molybdenum.* Materials Science and Engineering: A, 2020. **769**: p. 138511.
3. Vrancken, B., et al., *Heat treatment of Ti6Al4V produced by Selective Laser Melting: Microstructure and mechanical properties.* Journal of Alloys and Compounds, 2012. **541**: p. 177-185.
4. Xu, W., et al., *Additive manufacturing of strong and ductile Ti–6Al–4V by selective laser melting via in situ martensite decomposition.* Acta Materialia, 2015. **85**: p. 74-84.
5. Zafari, A., M.R. Barati, and K. Xia, *Controlling martensitic decomposition during selective laser melting to achieve best ductility in high strength Ti-6Al-4V.* Materials Science and Engineering: A, 2019. **744**: p. 445-455.
6. Motyka, M., *Martensite Formation and Decomposition during Traditional and AM Processing of Two-Phase Titanium Alloys—An Overview.* Metals - Open Access Metallurgy Journal, 2021. **11**: p. 481.
7. Mollamahmutoglu, M. and O. Yilmaz, *Volumetric heat source model for laser-based powder bed fusion process in additive manufacturing.* Thermal Science and Engineering Progress, 2021. **25**: p. 101021.
8. Mills, K.C., *Ti: Ti-6 Al-4 V (IMI 318)*, in *Recommended Values of Thermophysical Properties for Selected Commercial Alloys*, K.C. Mills, Editor. 2002, Woodhead Publishing. p. 211-217.
9. X. Gong, B.C., S. Price, K. Chou, *Powder-bed electron-beam-melting additive manufacturing: powder characterization, process simulation and metrology*, in *ASME Early Career Technical Conference (ECTC)*. 2013: District F. p. 59-66.
10. Parry, L., I.A. Ashcroft, and R.D. Wildman, *Understanding the effect of laser scan strategy on residual stress in selective laser melting through thermo-mechanical simulation.* Additive Manufacturing, 2016. **12**: p. 1-15.
11. Cho, J.Y., et al., *Selective laser melting-fabricated Ti-6Al-4V alloy: Microstructural inhomogeneity, consequent variations in elastic modulus and implications.* Optics & Laser Technology, 2019. **111**: p. 664-670.